CrossMark

ORIGINAL PAPER

Self-similarity and adaptive aperiodic stochastic resonance in a fractional-order system

Chengjin Wu · Shang Lv · Juncai Long · Jianhua Yang · Miguel A. F. Sanjuán

Abstract We investigate the aperiodic stochastic resonance (ASR) in a bistable fractional-order system when the fractional order lies in the interval (0, 2]. We find that a weak aperiodic signal can be amplified and optimized by varying the fractional order in the nonlinear system, no matter whether it has the assistance of the noise or not. We focus mainly on the self-similarity of the response to the input aperiodic signal and the adaptive ASR. The self-similarity is a characteristic that the response of a nonlinear system matches the input signal well, in the absence of the noise excitation. The adaptive ASR is a technique for the optimal ASR to occur by modulating the fractional order, the noise intensity, or the bistable system parameters. In order to make the optimal ASR occur, an adaptive particle swarm optimization (APSO) algorithm is used in this work as the method of parameter optimization. In previous works, only the periodic signal is optimized in a noisy bistable fractional-order system and the ASR induced by the fractional-order system has not been achieved. In engineering and scientific fields, not only periodic signals need to be processed, but also weak aperiodic ones. Moreover, the optimal ASR shows better results based on the APSO algorithm. We believe that the results of this paper might have a positive contribution in the dynamics research.

C. Wu · S. Lv · J. Long · J. Yang (✉)
School of Mechatronic Engineering, China University of Mining and Technology, Xuzhou 221116, China
e-mail: jianhuayang@cumt.edu.cn

J. Yang
Department of Mechanical Engineering, University of Michigan, Ann Arbor, MI 48109, USA

J. Yang
Jiangsu Key Laboratory of Mine Mechanical and Electrical Equipment, China University of Mining and Technology, Xuzhou 221116, China

M. A. F. Sanjuán
Nonlinear Dynamics, Chaos and Complex Systems Group, Departamento de Física, Universidad Rey Juan Carlos, Tulipán s/n, 28933 Móstoles, Madrid, Spain

M. A. F. Sanjuán
Department of Applied Informatics, Kaunas University of Technology, Studentu 50-407, Kaunas 51368, Lithuania

M. A. F. Sanjuán
Institute for Physical Science and Technology, University of Maryland, College Park, MD 20742, USA

🕿 Springer

1 Introduction

Stochastic resonance (SR) is a nonlinear physical phenomenon exploiting the effect of the background noise to enhance the system's response to a weak periodic input signal. The concept of SR was firstly proposed by Benzi et al. [1–3] to explain the periodic recurrence of ice ages on the earth in the early 1980s. Since the phenomenon of SR was discovered, it has attracted considerable attention over the past three decades and has been widely applied in physics [4], chemistry [5–7], biology [8–10], engineering [11–13], and so on. Furthermore, the theory of the adaptive SR [14] was proposed to achieve the SR optimality condition and it is widely applied in many disciplines [15,16]. However, given that real-world external signals are typically aperiodic, the applicability of SR to a practical project is limited to some extent. Another interesting phenomenon consisting in the fact that noise can also serve to enhance the response of a nonlinear system to a weak aperiodic input signal was found by Collins et al. [17–19]. It is called aperiodic stochastic resonance (ASR). ASR can be used to detect and process weak aperiodic signals. Also, the ASR technique has been used to implement memory and logic gates [20], baseband binary signal transmission [21–24], mammalian cutaneous mechanoreceptors [25], digital watermarking [26], optical cavity [27], etc. The bipolar binary signal is one kind of common aperiodic signal. It is usually utilized in the field of information transmission and other signal issues. Studying on it may be benefit to improve the accuracy of digital communication and pattern recognition. Moreover, it has been investigated by both experimental [28–30] and numerical methods [31,32]. As a result, the bipolar binary signal will be considered in this paper.

In recent years, due to the intensive development of fractional-order calculus theory, there have been several researches on the phenomenon of SR in fractional-order nonlinear systems [33–35]. As expected, SR can also occur as a response by modulating the fractional order, noise intensity, or system parameters. More importantly, fractional-order systems usually show better properties. It especially has excellent performance in industrial control [36,37], viscoplasticity modeling [38,39], signal processing [40], mechanical fault diagnosis [41], membrane mechanics [42], and in many other fields. Moreover, under the excitation of periodic signals, the fractional systems may present rich dynamical behaviors. Shen et al. [43,44] studied the primary and subharmonic resonance of the van der Pol oscillator with fractional-order derivative by the averaging method and discussed the effects of the fractional damping. Yang and Zhu [45] investigated the vibrational resonance phenomenon in overdamped and underdamped Duffing systems with fractional-order damping. Some new resonance and bifurcation phenomena were found.

Although some interesting results have been reported in many research articles, some problems still need to be further discussed. On the one hand, external weak signals, which we need to process, are usually aperiodic in the real world. Hence, it is necessary to achieve the ASR induced by the nonlinear system. Meanwhile, in view of better properties of the fractional-order system, in this work, we will analyze some dynamical properties of ASR in a noisy bistable fractional-order system when the fractional-order lies in the interval (0, 2). On the other hand, the adaptive SR was applied in different fields, but the adaptive ASR has not been achieved. In addition, the response of a nonlinear system subjected to only a weak aperiodic input signal has not been intensively studied yet.

The rest of this paper is organized as follows. In Sect. 2, we will investigate the properties of the response of a nonlinear system induced by an aperiodic input signal. Besides, we will introduce an index to discuss the self-similarity of the response to the input signal. In Sect. 3, we will investigate the phenomena of the traditional ASR induced by the fractional order and the noise intensity, respectively. In Sect. 4, we will make the optimal ASR occur based on the adaptive particle swarm optimization (APSO) algorithm. Finally, we will give main conclusions of this paper in Sect. 5.

2 Self-similarity of the response to the input aperiodic signal

A typical fractional-order system is governed by

$$\frac{\mathrm{d}^\alpha x}{\mathrm{d}t^\alpha} = f(x) + s(t), \quad \alpha \in (0, 2], \tag{1}$$

where $f(x)$ is a nonlinear function and $s(t)$ is an aperiodic signal. In this paper, we let $f(x) = ax - bx^3$ which is a bistable potential system. Herein, we use the Grünwald–Letnikov definition [46,47] for the

fractional-order differential operator to discretize the fractional-order system. According to the Grünwald–Letnikov definition, the fractional-order differential operator is defined as follows

$$\frac{d^\alpha x(t)}{dt^\alpha}\bigg|_{t=kh} = \lim_{h\to 0}\frac{1}{h^\alpha}\sum_{j=0}^{k}(-1)^j\binom{\alpha}{j}x(kh-jh),$$

(2)

where h denotes the time step and $\binom{\alpha}{j}$ is the binomial coefficient

$$\binom{\alpha}{j} = \frac{\Gamma(\alpha+1)}{\Gamma(j+1)\Gamma(\alpha-j+1)}.$$

(3)

In Eq. (3), $\Gamma(\bullet)$ is the Gamma function. Letting $w_j^\alpha = (-1)^j\binom{\alpha}{j}$, according to [47], we have

$$w_0^\alpha = 1, \quad w_k^\alpha = \left(1 - \frac{\alpha+1}{k}\right)w_{k-1}^\alpha, \quad k = 1, 2, \ldots, n.$$

(4)

Under the zero initial conditions, the fractional-order operator is discretized to

$$\frac{d^\alpha x(t)}{dt^\alpha}\bigg|_{t=kh}$$
$$= \lim_{h\to 0}\frac{1}{h^\alpha}\left[x(kh) + \sum_{j=1}^{k-1}w_j^\alpha x(kh-jh)\right]. \quad (5)$$

For simplification, we introduce the notation as $x_k = x(kh)$. Here, x_k is the kth point in the discrete time series. For a small value of h, the limitation symbol can be removed. As a result, we get the discretization for Eq. (1), i.e.,

$$x_k = -\sum_{j=1}^{k-1}w_j^\alpha x_{k-j} + h^\alpha[f(x_{k-1}) + s_{k-1}].$$

(6)

In this paper, $s(t)$ is the aperiodic bipolar binary signal

$$s(t) = A\sum_{i=0}^{\infty}q_i\Gamma(t-iT)$$
$$\Gamma(t) = \begin{cases} 1, & t \in [0, T] \\ 0, & t \notin [0, T] \end{cases}.$$

(7)

Herein, A is the signal amplitude and T is the minimal random pulse width. Besides, q_i presents the random numbers of $+1$ or -1 with an independent distribution.

The input signal and the output signal of Eq. (1) under the fractional-order value $\alpha = 0.1, 0.5, 1, 1.5, 2$ are, respectively, given in Fig. 1 by the algorithm shown in Eq. (6). In Fig. 1b, when the fractional order $\alpha = 0.1$, the signal distortion appears. In Fig. 1c, as the fractional order increases to $\alpha = 0.5$, the distortion of the output signal turns severely. With the increase in the fractional order further, as shown in Fig. 1d, e, $\alpha = 1.0$ and $\alpha = 1.5$, respectively, the distortion of the output signal compared with the input signal turns slightly. If we continue to increase α to 2, as shown in Fig. 1f, the output presents oscillation behavior. There are some monographs investigating this kind of oscillation according to the nonlinear vibration theory [48,49], where the signals are distorted completely for this case.

To measure the strength of the output, we define an index β as the amplification factor, specifically,

$$\beta = \frac{\frac{1}{n}\sum_{k=1}^{n}|x_k - \bar{x}|}{A}.$$

(8)

In Eq.(8), the term $\bar{x} = \frac{1}{n}\sum_{k=1}^{n}x_k$ is the mean value of the response. Another term $|x_k - \bar{x}|$ represents the distance of the kth point to the mean value of the response. Further, the numerator in Eq. (8), i.e., the term $\frac{1}{n}\sum_{k=1}^{n}|x_k - \bar{x}|$ is an approximate ensemble mean value of the response amplitude. We know that the time series appear around the mean value of the response. Hence, Eq. (8) represents the ratio of the amplitude of the output to the input approximately. We declare that β defined in Eq. (8) is only an approximate measurement. Due to the stochastic characteristics of an aperiodic signal, it is difficult to give a definition to measure the amplitude of the response exactly. When $t \to \infty$, β approaches an exact value.

To investigate the influence of the fractional order on the response of the bistable system, we plot the dependence of the amplification factor β on the value of the fractional order α in Fig. 2a. Apparently, with the increase in the fractional order, the magnitude of the amplification factor begins to increase gradually, then it almost keeps changeless when the fractional order reaches a certain value. In addition, it can be seen clearly that the smaller the signal amplitude is, the larger the amplification factor will be. In other words,

Fig. 1 **a** The input signal.
b–f The response of the
system under different
values of the fractional
order. The simulation
parameters are $a = 0.2$,
$b = 0.2$, $A = 0.2$, $h = 0.1$,
$T = 100$, in **b** $\alpha = 0.1$, in **c**
$\alpha = 0.5$, in **d** $\alpha = 1$, in **e**
$\alpha = 1.5$, and in **f** $\alpha = 2$
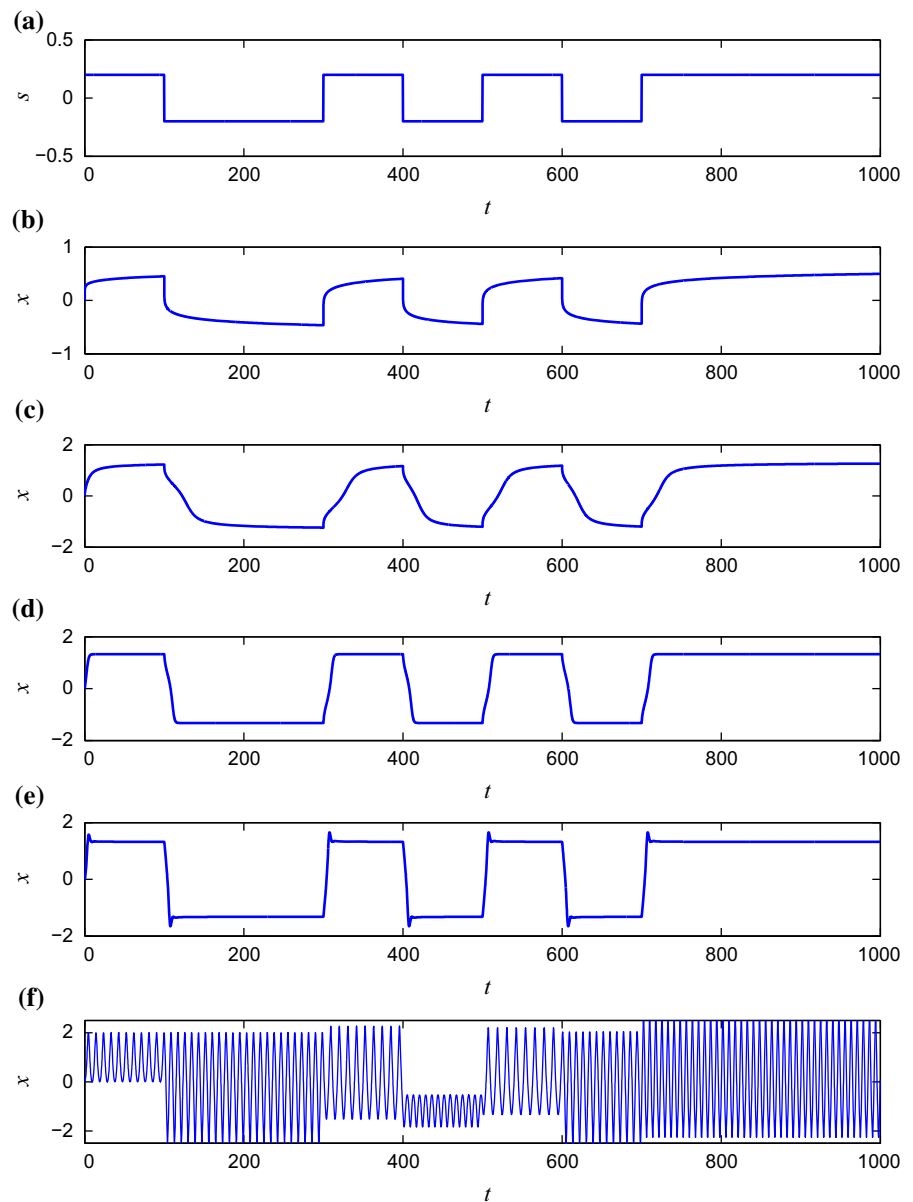
the weak aperiodic signal can be enhanced by the frac-tional order system easily.

From Fig. 1, we learn that the distortion of the out-put signal is influenced by the factional-order. From the time series, we cannot measure the distortion quantita-tively. Hence, we introduce the cross-correlation coef-ficient which is a common index in the statistics and an effective tool to describe the similarity of two differ-ent time series. The cross-correlation coefficient C_{sx} which measures the similarity between the input signal and the output signal is given by

$$C_{sx} = \frac{\sum_{k=1}^{n}(s_k - \bar{s})(x_k - \bar{x})}{\sqrt{\sum_{k=1}^{n}(s_k - \bar{s})^2 \sum_{k=1}^{n}(x_k - \bar{x})^2}}, \qquad (9)$$

where s_k is the kth point in the signal time series and $\bar{s} = \frac{1}{n}\sum_{k=1}^{n} s_k$. The notation $\bar{x}$ is the same as that defined in Eq. (8).

In Fig. 2b, we give curves of the cross-correlation coefficient C_{sx} versus the fractional order α. With the increase of α, C_{sx} goes down gradually. However, when C_{sx} decreases to a certain value, C_{sx} goes up to the

(a)

(b)
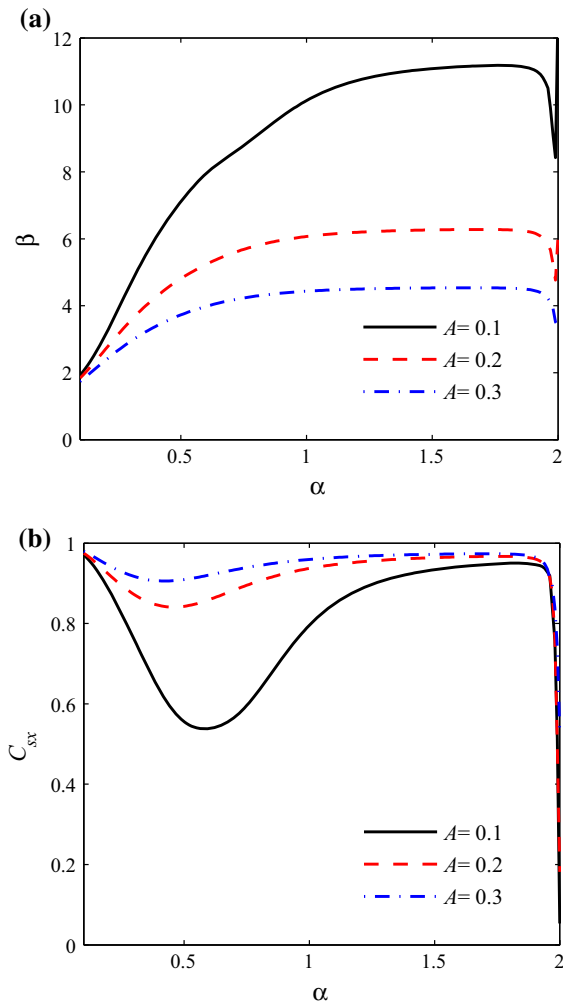
Fig. 2 **a** The magnitude of the amplification factor versus the fractional order for different values of the amplitude. **b** The cross-correlation coefficient versus the fractional order for different values of the amplitude. The simulation parameters are $a = 0.2$, $b = 0.2$, $A = 0.2$, $h = 0.1$ and $T = 100$

maximal value and keeps it as a constant almost before $\alpha = 2$. For small values of α, the distortion is slight. It can also be obtained from the time series in Fig. 1b intuitively. However, it is a remarkable fact that the cross-correlation coefficient goes down dramatically and reaches a very small value when the fractional order α approaches to 2 closely. It is because the oscillation appears for this case as shown in Fig. 1f. In other words, the curves in Fig. 2b can express the distortion of the time series excellently. Consequently, from Figs. 1 and 2b, we can see that the cross-correlation coefficient is an effective tool to characterize the degree of the sig-

nal distortion. Moreover, we find that the smaller the signal amplitude is, the smaller of the maximal value of C_{sx} will be. It is contrary to the effect of the signal amplitude on the amplification factor in Fig. 2a.

To help understand the performance of the fractional-order system further, we give some explanations with the help of the considered system under the step signal excitation. It is because in a short-time interval, the system under the aperiodic binary signal excitation may be viewed as that under a step signal excitation. The step response curves of the fractional-order system for several values of α are illustrated in Fig. 3. When $\alpha \leq 1$, for example $\alpha = 0.1, 0.5, 1$, the response is sluggish without oscillation and does not overshoot the mean value of the response. As α increases, the mean value of the response also increases in Fig. 3b. The amplitude of the response is controlled by fractional order in certain range, which is the same as the phenomenon of Fig. 1. As α increases over 1, for example $\alpha = 1.5, 1.8$, the response overshoots and oscillates around the final value. The larger α is, the larger of the overshoot is and the longer it takes for the oscillations to die out. As α increases to 2, the oscillation is sustained. These facts are in accordance with those in Fig. 1b–f. Hence, taking Figs. 1 and 3 into account, we educe that the waveform of the output is mainly affected by the transient response and the amplitude of the output is mainly affected by the fractional order. As to the focus in this paper, i.e., the similarity and the amplification of the signal, the response of the system induced by the transition of the aperiodic signal from negative (positive) to positive (negative) value is the key factor. In the transition point, the performance of the system under the excitation of aperiodic bipolar binary signal is similar to that under the excitation of a step signal. Hence, as we show in Fig. 3, the factional-order value influences the waveform and amplitude, i.e., the performance of the system.

To investigate the dependence of the response on the input signal thoroughly, we keep the signal amplitude fixed, but change the signal waveform only. In Fig. 4, three aperiodic signals for different waveforms with $A = 0.1$ are given. Then, we plot Fig. 5 under the excitation of these signals. In Fig. 5a, the curves of the amplification factor β versus the fractional order α are plotted. In this subplot, we see that the $\beta - \alpha$ curve is independent of the input signal waveform. In Fig. 5b, the curves of the cross-correlation coefficient C_{sx} versus the fractional order α are shown. Apparently, the

Fig. 3 **a** The step response
of the fractional-order
system for several values of
the fractional order. **b** The
mean value of the step
response versus the
fractional order. The
simulation parameters are
$a = 0.2$, $b = 0.2$, $A = 0.2$,
$h = 0.1$ and $T = 100$
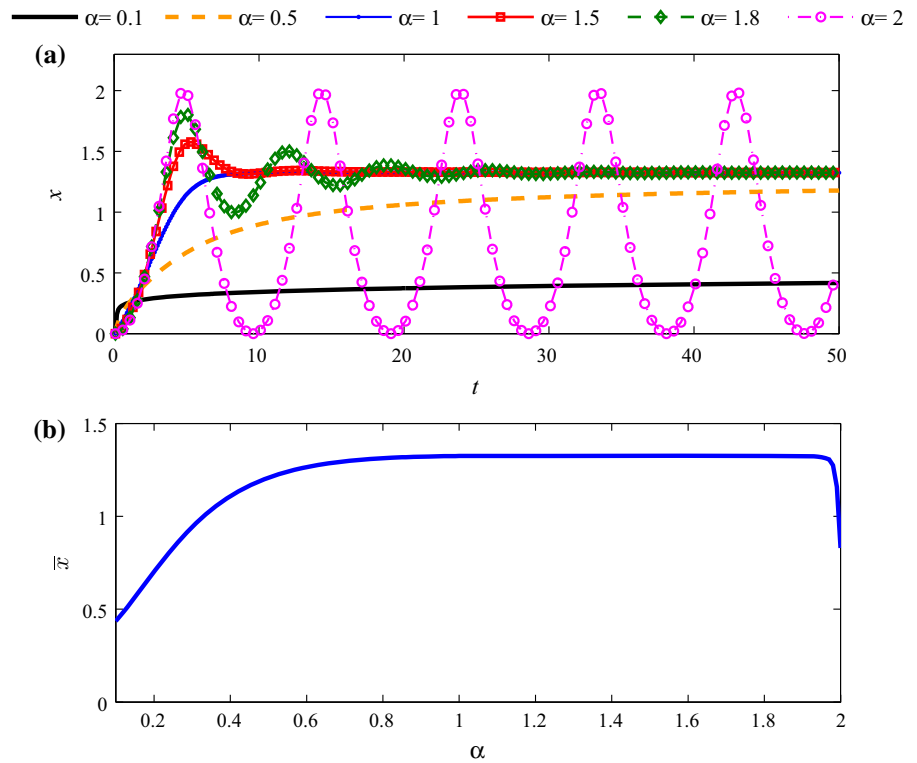
Fig. 4 The input aperiodic
signal for three different
waveforms with $A = 0.1$
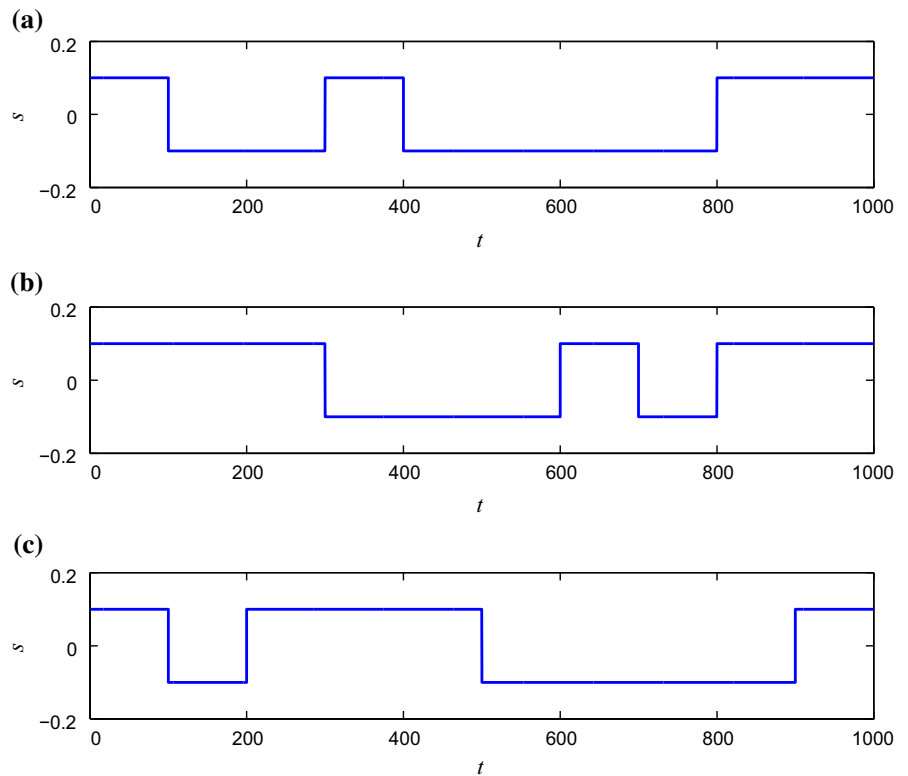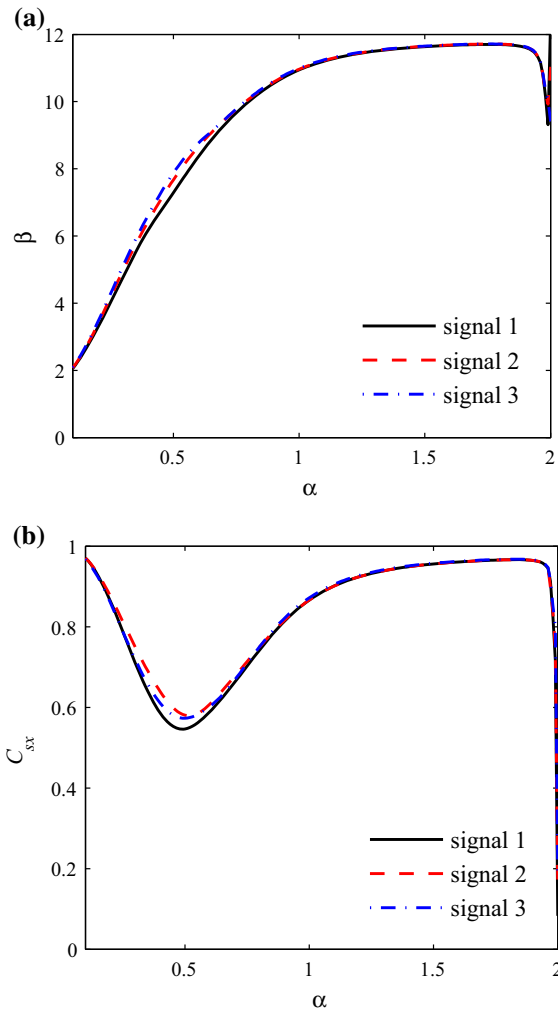
Fig. 5 a The amplification factor versus the fractional order under the excitation of three input signals described in Fig. 4. **b** The cross-correlation coefficient versus the fractional order under the excitation of three input signals described in Fig. 4. The simulation parameters are $a = 0.2$, $b = 0.2$, $A = 0.1$, $h = 0.1$ and $T = 100$

$C_{sx} - \alpha$ curve is also independent of the input waveform. These facts reveal that the dynamical properties (such as β and C_{sx}) of the response is almost independent of the waveform of the aperiodic signal. However, in Fig. 2, we know that these dynamical properties closely depend on the signal amplitude.

As a conclusion of this section, we find that the output of the system can be optimized and amplified by modulating the fractional-order value. The main properties of the response are independent of the signal waveform but influenced by the signal amplitude.

Moreover, the cross-correlation coefficient introduced in this section is an effective index to measure the signal distortion.

3 The noise-induced traditional ASR

Noise is almost ubiquitous in nature. The SR induced by a noisy bistable system has been investigated in our previous work [50]. Even though some interesting results have been observed, it is significant to investigate the ASR induced by a nonlinear system, since the ASR is a high efficient method to process the aperiodic signal. To our knowledge, the ASR has not yet been achieved in a fractional-order system. Hence, it is necessary to study and develop the ASR further, especially in a fractional-order system.

As is well known, the fractional-order damping and the noise are important factors to induce the SR phenomenon [50]. Hence, we focus mainly on how the fractional-order value and noise intensity affect the ASR phenomenon in the following. In this part, the system for ASR to occur is a typical nonlinear system which is governed by

$$\frac{\mathrm{d}^\alpha x}{\mathrm{d}t^\alpha} = f(x) + s(t) + \xi(t), \quad \alpha \in (0, 2], \tag{10}$$

where we still use $f(x) = ax - bx^3 \cdot s(t)$ is an aperiodic signal function as is used in last section. $\xi(t)$ is a Gaussian white noise with the following statistical properties

$$\langle \xi(t) \rangle = 0, \quad \langle \xi(t_1)\xi(t_2) \rangle = \sigma^2 \delta(t_1 - t_2). \tag{11}$$

In Eq. (11), σ is the noise intensity. According to [51], the time series of a Gaussian white noise can be constructed by the following series

$$\xi_k = \frac{\sigma}{\sqrt{h}}\zeta_k, \quad k = 1, 2, \ldots, n, \tag{12}$$

where ζ presents the random numbers with the standard normal distribution and h represents the time step. Similar to the deducing process from Eqs. (1) to (6), we obtain the discretization algorithm for Eq. (10)

$$x_k = -\sum_{j=1}^{k-1} w_j^\alpha x_{k-j} + h^\alpha [f(x_{k-1}) + s_{k-1} + \xi_{k-1}]. \tag{13}$$
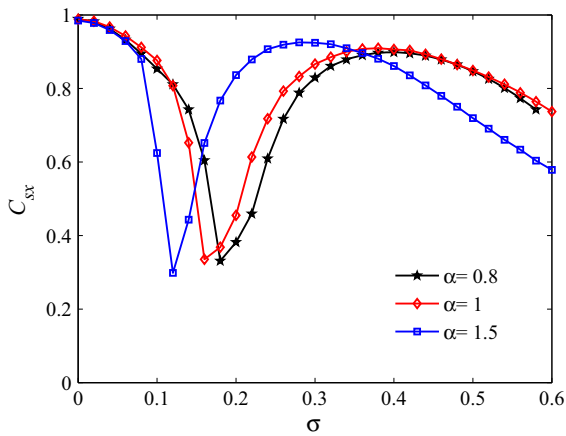
Fig. 6 The cross-correlation coefficient versus the noise intensity for different fractional-order values. The simulation parameters are $a = 1, b = 1, A = 0.22, h = 0.2$ and $T = 200$
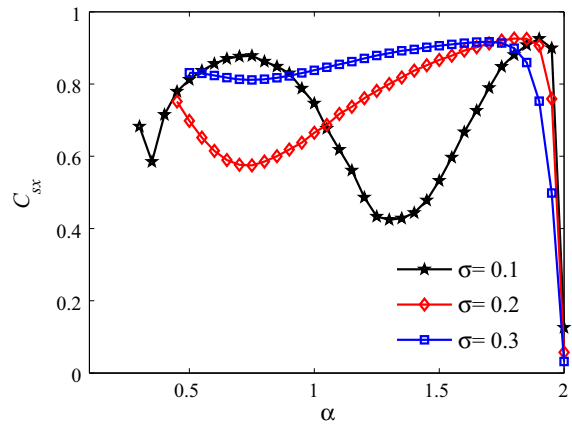
Fig. 8 The cross-correlation coefficient versus the fractional order for different values of the noise intensity. The simulation parameters are $a = 1, b = 1, A = 0.3, h = 0.1$ and $T = 100$

The response of the fractional system under the aperiodic signal and noise excitation can be calculated by using Eq. (13).

In Fig. 6, we fix the fractional order α as a constant, for example $\alpha = 0.8$, the noise intensity on the response of the fractional-order system is shown

Fig. 7 **a** The input aperiodic signal. **b–d** The response of the system under different noise intensities with $\alpha = 1.5$. The simulation parameters are $a = 1, b = 1, A = 0.22$, $h = 0.2, T = 200$, in **b** $\sigma = 0.1$, in **c** $\sigma = 0.3$, and in **d** $\sigma = 0.6$
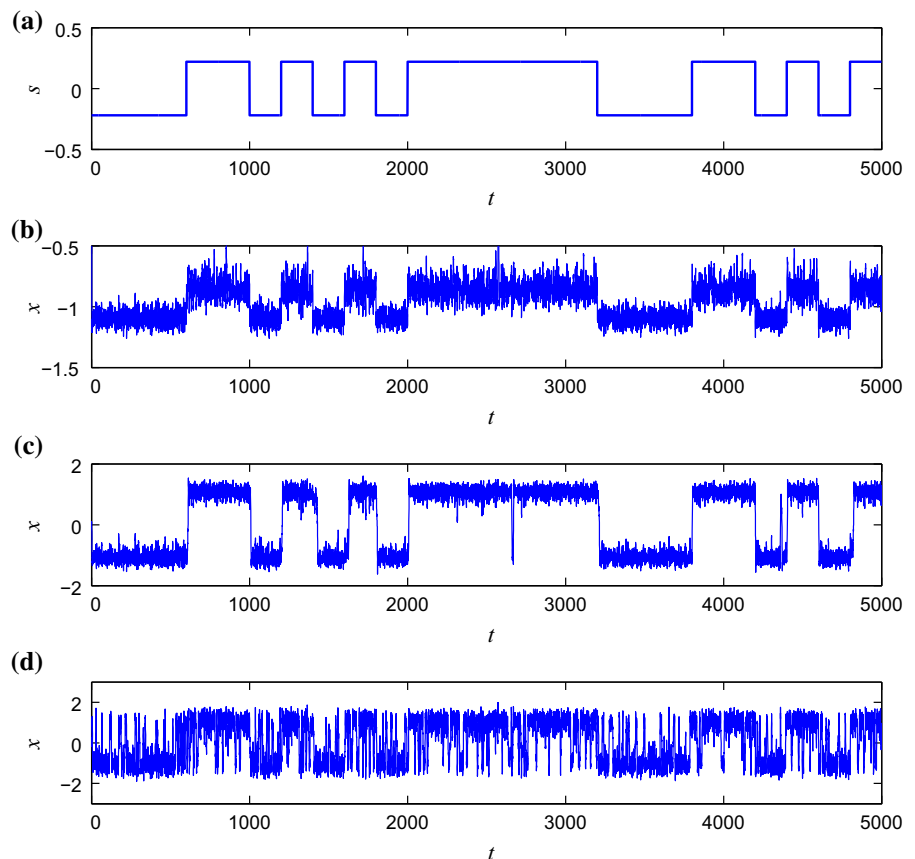
Fig. 9 **a** The input
aperiodic signal. **b–e** The
response of the system
under different
fractional-order values with
$\sigma = 0.1$. The simulation
parameters are $a = 1$,
$b = 1$, $A = 0.3$, $h = 0.1$,
$T = 100$, in **b** $\alpha = 0.4$, in **c**
$\alpha = 0.7$, in **d** $\alpha = 1.3$, in **e**
$\alpha = 1.9$, in **f** $\alpha = 1.98$
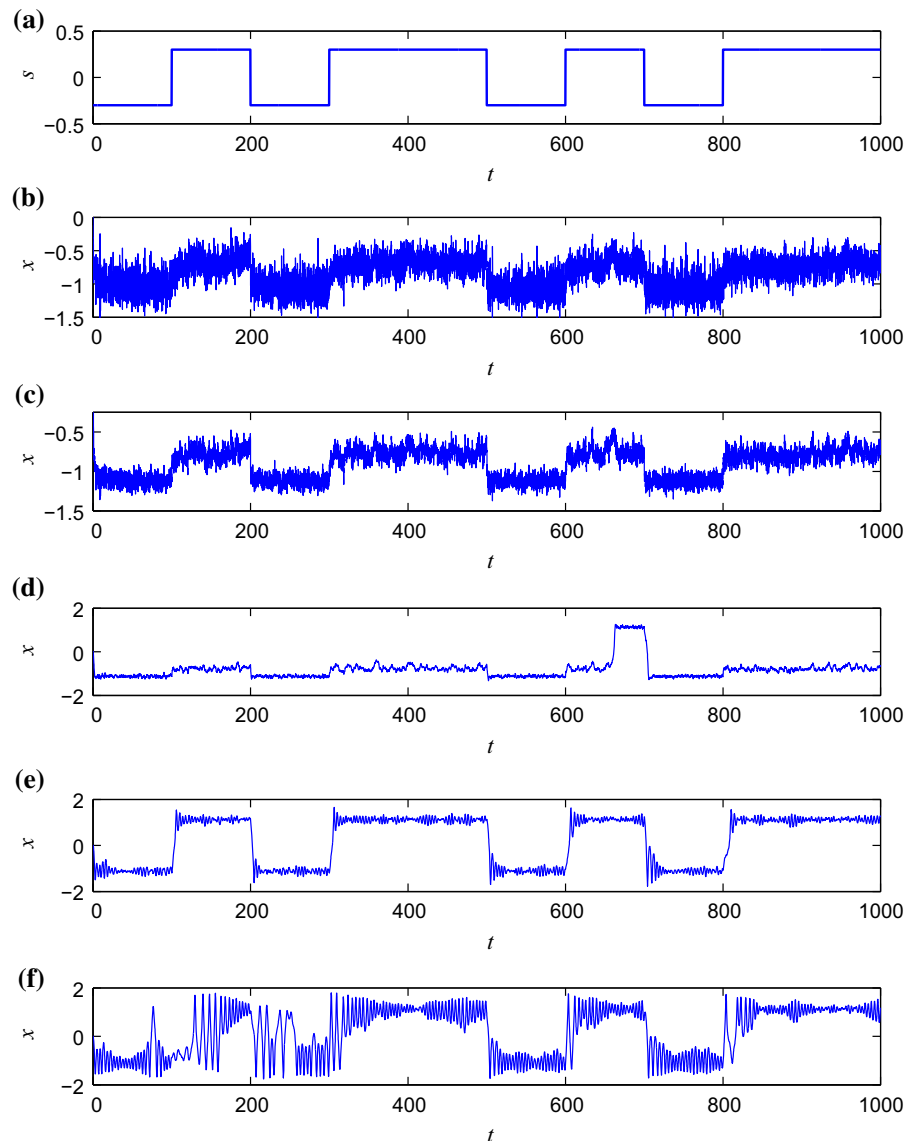
clearly. It can be seen that the change tendency of the curves in the fractional-order system is similar to that in the ordinary system ($\alpha = 1$). Corresponding to the curve (for $\alpha = 1.5$) in Fig. 6, different time series of the fractional-order system under a Gaussian white noise excitation are given in Fig. 7. We use the same aperiodic input signal in Figs. 6 and 7. The input aperiodic signal is shown in Fig. 7a. We see that the weak input signal is optimized and amplified in a nonlinear fractional-order system when $\sigma = 0.3$, as shown in Fig. 7c. In other words, $\sigma = 0.3$ is the optimal noise intensity. Under weaker noise excitation, the output signal turns worse,

as shown in Fig. 7b, although C_{sx} can reach a quite high value. Under stronger noise excitation, the weak input signal will be overwhelmed by the noise and the output is scrambled, as shown in Fig. 7d. Moreover, based on the fact that the larger the fractional order is, the smaller the optimal noise intensity will be, the ASR tends to occur more easily. It can also be seen from Fig. 6. In other words, there exists a reference value of the parameter modulation to achieve optimal ASR. Both Figs. 6 and 7 show the traditional ASR induced by modulating the noise intensity.
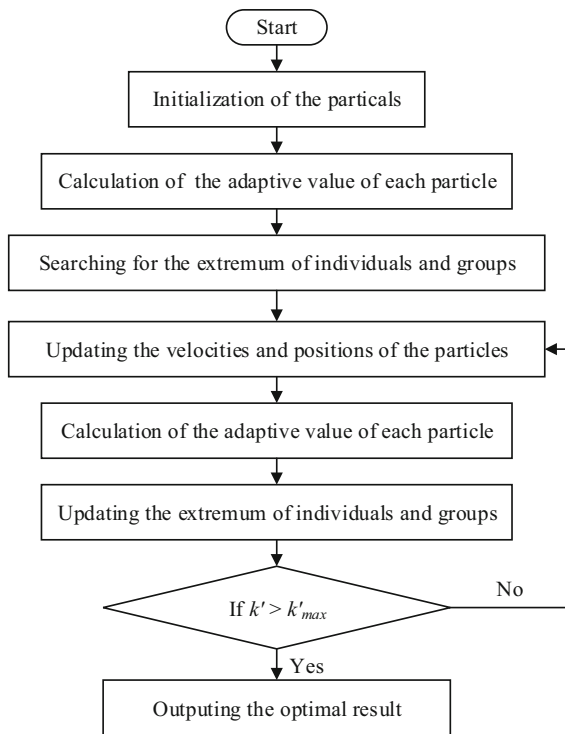
Fig. 10 The flowchart for the adaptive ASR based on the APSO algorithm

To investigate the effect of the fractional order on the response of the fractional-order system, we fix the noise intensity and make the fractional order as a controllable variable. The cross-correlation coefficient C_{sx} versus the fractional order α is clearly shown in Fig. 8. For the case $\sigma = 0.1$, the $C_{sx} - \alpha$ curve presents apparently a double-peak. However, when the noise intensity is $\sigma = 0.2$, the cross-correlation coefficient function degenerates into a single peak. If we increase the noise intensity further, the curve of the cross-correlation coefficient function tends to be flat. In other words, the effect of the fractional order on the response will be weaker, when the noise intensity increases gradually. In addition, for the case $\sigma = 0.1$, in the intervals

[0.3, 0.7] and [1.3, 1.9], the cross-correlation rises with the increase of α. However, in the intervals (0.2, 0.3], [0.7, 1.3] and [1.9, 2], the cross-correlation decreases with the increase of α. Corresponding to the curve (for the case $\sigma = 0.2$) in Fig. 8, the time series of five output signals are depicted in Fig. 9. We use the same aperiodic input signal in Figs. 8 and 9. The input aperiodic signal is shown in Fig. 9a. In Fig. 9c, $\alpha = 0.7$, it corresponds to the first peak of the curve in Fig. 8. In Fig. 9e, $\alpha = 1.9$, it corresponds to the second peak of the curve in Fig. 8. In Fig.9d, the optimal output is achieved. For other fractional-order values, such as time series in Fig. 9b–d, the output cannot cross the potential well synchronically with the input signal. The output signals are distorted for these cases.

As a conclusion of this section, we find that both the noise intensity σ and the fractional order α can induce the ASR. Moreover, the ASR induced by the noise can improve the cross-correlation coefficient and reduce the signal distortion effectively. In other words, the noise-induced ASR plays an important role in the fidelity of the input signal. Moreover, we find that the larger the fractional order is, the smaller the optimal noise intensity might be.

4 The adaptive ASR

The adaptive SR is a theory for the optimal SR to occur by modulating the fractional order, noise intensity, or system parameters. Similarly, the adaptive ASR is to achieve an optimal ASR by modulating the related parameters. In order to search these optimal parameters fast and exactly, we can utilize some optimization algorithms, such as the particle swarm optimization (PSO) algorithm [52], the modified particle swarm optimization algorithm [53], and the genetic algorithm [54].

The APSO algorithm [55] possesses better search efficiency than the classical PSO, especially performing a global search over the entire search space with a

Table 1 The optimization results of the fractional order and the noise intensity under different values of the system parameter a

a	0.1	0.3	0.5	0.6	0.8	1	1.2
α	1.087280	1.404065	1.591632	1.644298	1.844786	1.462384	1.556489
σ	0.200682	0.208095	0.202791	0.210723	0.200462	0.385922	0.436082
C_{sx}	0.937289	0.945958	0.947071	0.925858	0.888732	0.840848	0.785853

The simulation parameters are $b = 0.8$, $A = 0.2$ and $T = 100$

Fig. 11 a The input
aperiodic signal. **b–d** The
response of the system
under the noise excitation
with different values of the
system parameter. The
simulation parameters are
$b = 0.8$, $A = 0.2$, $h = 0.1$,
$T = 100$, in **b** $a = 0.3$, in **c**
$a = 0.6$, and in **d** $a = 0.8$
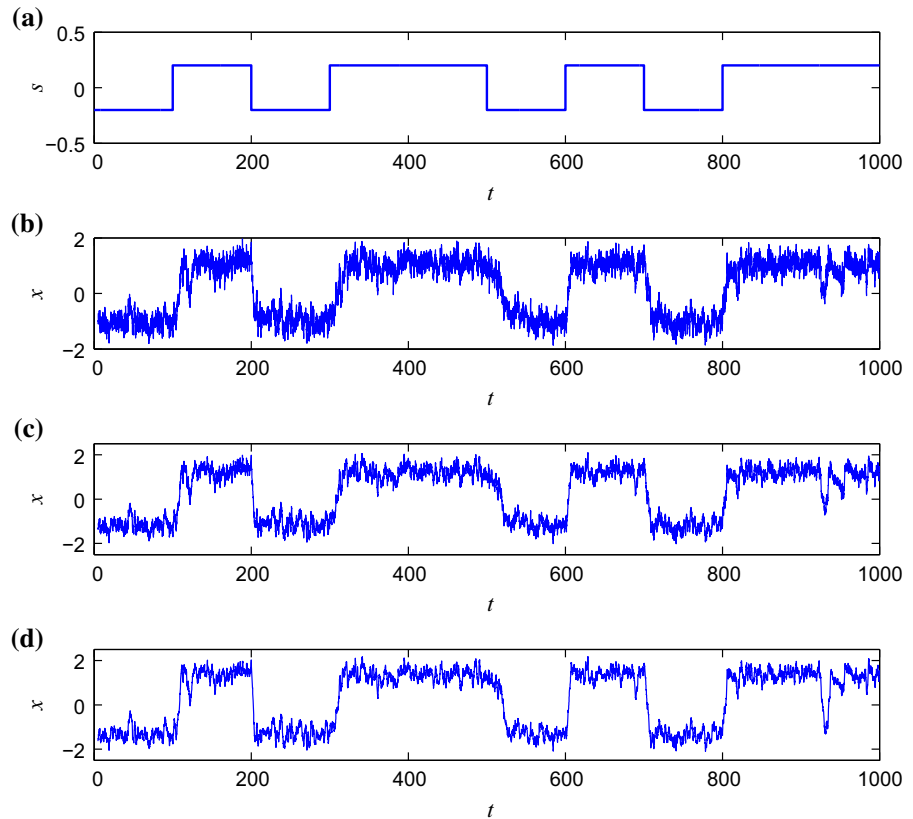
Table 2 The optimization results of the system parameters under different values of the fractional order

α	0.6	0.7	0.8	1.0	1.2	1.4	1.6
a	0.548526	0.444167	0.296858	0.234842	0.312448	0.399378	0.344482
b	0.652437	0.529641	0.361056	0.237422	0.226623	0.213681	0.149553
C_{sx}	0.800489	0.832314	0.850076	0.867303	0.872182	0.870035	0.865829

The simulation parameters are $\sigma = 0.36$, $A = 0.2$, $h = 0.1$ and $T = 100$

faster convergence speed. The classical PSO algorithm
can easily get trapped in the local optima when solving
complex multimodal problems. Hence, we choose the
APSO algorithm as the optimization method.

Each particle is regarded as a potential solution to
a problem. The ith particle is connected with two vec-
tors, i.e., the position and velocity of the particle. The
position of the ith particle is recorded as the vector
$\mathbf{X_i} = (x_{i1}x_{i2},\ldots x_{id}), i = 1, 2, \ldots m$. The veloc-
ity of the particle i is recorded as the vector $\mathbf{V}_i =
(v_{i1}, v_{i2}, \ldots v_{id}), i = 1, 2, \ldots m$. Here, d stands for
the dimensions of the search space. At first, each parti-
cle with random position and velocity on d dimensions
is initialized. The initial fitness value of each particle is

obtained by using the fitness function $g(x)$. $\mathbf{P}_{id}$ is the
local best value of the position and $\mathbf{P}_{gd}$ is the global
best value of the position. They are governed by

$$p_{id}(k' + 1)$$
$$= \begin{cases} p_{id}(k'), & g(x_{id}(k' + 1)) < g(p_{id}(k')) \\ x_{id}(k' + 1), & g(x_{id}(k' + 1)) \geq g(p_{id}(k')) \end{cases} \quad (14)$$

and

$$p_{gd}(k' + 1)$$
$$= \begin{cases} p_{gd}(k'), & g(p_{id}(k' + 1)) < g(p_{gd}(k')) \\ p_{id}(k' + 1), & g(p_{id}(k' + 1)) \geq g(p_{gd}(k')) \end{cases}, \quad (15)$$

where k' represents the k'th iteration ($k' < k'_{\max}$). $k'_{\max}$
represents the maximum value of the iterations. As a

Fig. 12 a The input
aperiodic signal. **b–d** The
response of the system
under the noise excitation
with different values of the
fractional order. The
simulation parameters are
$\sigma = 0.36$, $A = 0.2$,
$h = 0.1$, $T = 100$, in **b**
$\alpha = 0.8$, in **c** $\alpha = 1$, and in
d $\alpha = 1.2$
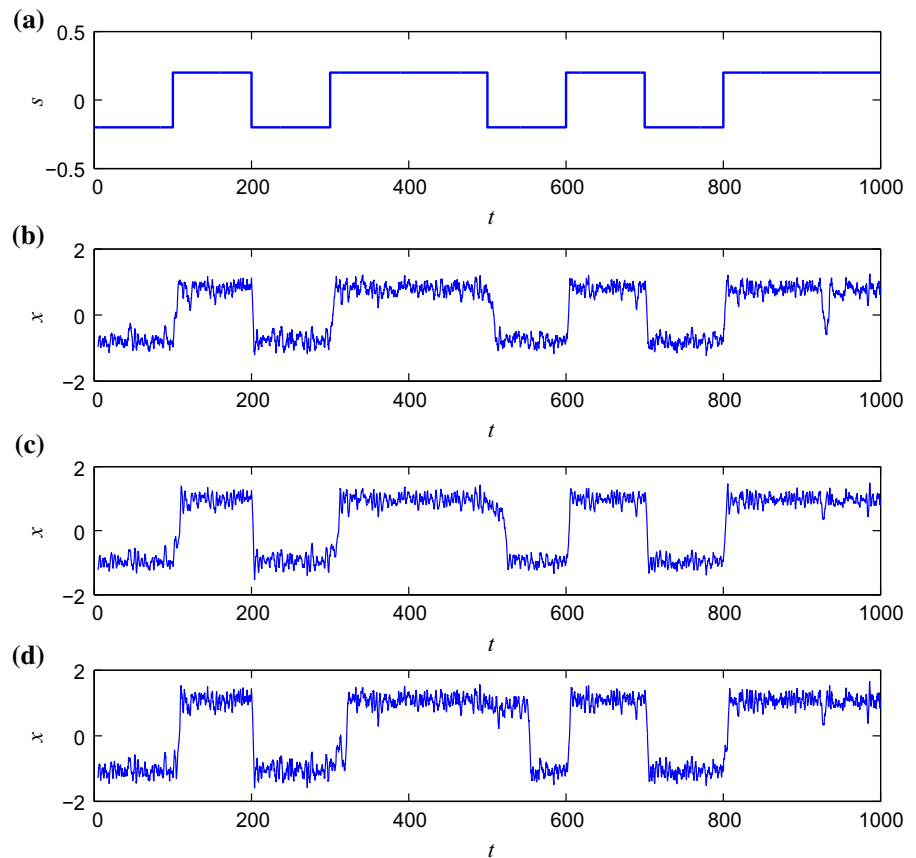
result, $\mathbf{P}_{id}$ equals $\mathbf{P}_{gd}$ when $k' = 0$, which is the best
value of the initial fitness values of all particles. The
position and velocity of each particle are updated as

$$x_{id}(k' + 1) = x_{id}(k') + v_{id}(k' + 1) \tag{16}$$

and

$$v_{id}(k' + 1) = wv_{id}(k') + c_1 r_1 [p_{id}(k') - x_{id}(k')] \\ + c_2 r_2 [p_{gd}(k') - x_{id}(k')], \tag{17}$$

where c_1 and c_2 are acceleration constants, as well as
r_1 and r_2 are the random numbers in the interval $[0, 1]$.
In Eq. (18), w represents the inertia weight controlling
the effect of the former velocity on the present velocity.
We can modulate w to skip the local minimum. It can
be determined by

$$w = \begin{cases} w_{\min} - \frac{(w_{\max} - w_{\min})(g - g_{\min})}{g_{\text{avg}} - g_{\min}}, & g \le g_{\text{avg}} \\ w_{\max}, & g > g_{\text{avg}} \end{cases} \tag{18}$$

Herein, $w_{\max}$ represents the maximum of w, and $w_{\min}$
represents the minimum of w, as well as g represents
the present fitness function value of the particle. In
addition, g_{avg} and $g_{\min}$ are the average value and the
minimum value of the entire particle swarm. Then, the
flowchart for the adaptive ASR based on the APSO
algorithm is depicted in Fig. 10.

In the following section, we will achieve the opti-
mal ASR based on the APSO algorithm. The nonlinear
function is still in the form $f(x) = ax - bx^3$. In addi-
tion, the cross-correlation coefficient C_{sx} is the fitness
function here.

Firstly, we fix the parameter $b = 0.8$, but take the
fractional order and the noise intensity as the targets
of the global optimization under different values of the
parameter a. The results of the global optimization are
shown in Table 1. Moreover, according to the results,
the responses of a fractional-order system under differ-
ent values of a are given in Fig. 11. We can observe
the ASR clearly and make it occur based on the APSO
algorithm.
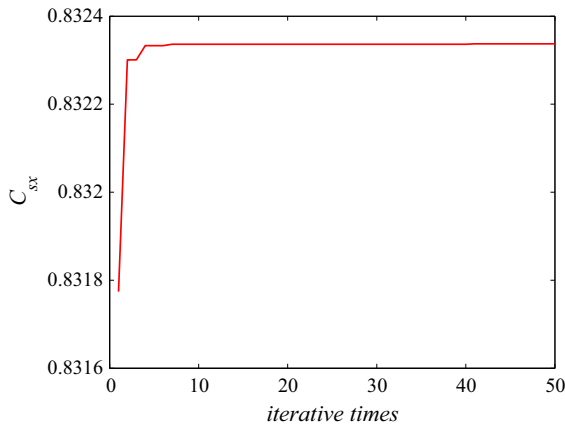
Fig. 13 The convergence curve of the APSO algorithm

Secondly, we fix the parameter $\sigma = 0.36$, but take the system parameters a and b as the targets of the global optimization under different values of the fractional order α. The results of the global optimization are shown in Table 2. In addition, according to the results, some time series of the fractional-order system under different values of α are plotted in Fig. 12. Similarly, the phenomenon of the ASR also appears.

Finally, we plot the convergence curve of the APSO algorithm in an numerical experiment, as shown in Fig. 13. We can see that the optimal results can be obtained when $k' = 7$. It takes us about 485 s to obtain the optimal results in a simple and accurate manner by our laptop.

5 Conclusions

In this work, we have investigated the ASR in a fractional-order bistable system induced by a Gaussian white noise. We focus mainly on two points in this paper: the properties of the response of a nonlinear system excited by aperiodic input signals and the ASR induced by the noise intensity and the fractional order. In addition, we achieve the adaptive ASR based on the APSO algorithm.

With regard to the first problem, we find that the weak input signals can be amplified and optimized by the system only depending on modulating the fractional-order value. However, these properties are independent of the waveform of the input signal, except the amplitude. Moreover, we utilize the cross-

correlation coefficient to characterize the degree of the signal distortion and it works well.

For the second problem, we investigate the ASR induced by a fractional-order system. Both the fractional order and the noise intensity can induce ASR. For a fixed fractional order, ASR occurs by modulating the noise intensity. For a fixed noise intensity, ASR can also occur by tuning the fractional order. Moreover, we find that the larger the fractional order is, the smaller the optimal noise intensity might be.

Finally, we achieve the optimal ASR based on the APSO algorithm. Taking the noise intensity and fractional order as the targets of optimization, the optimal ASR can occur. Taking the system parameters as the targets of optimization, ASR can also occur. We believe that the APSO algorithm might have a positive value in the dynamics research, performing a global search over the entire search space with a fast convergence speed.

References

1. Benzi, R., Sutera, A., Vulpiani, A.: The mechanism of stochastic resonance. J. Phys. A Math. Gen. **14**, L453–L457 (1981)
2. Benzi, R., Parisi, G., Sutera, A., Vulpiani, A.: Stochastic resonance in climatic change. Tellus **34**, 10–16 (1982)
3. Benzi, R., Parisi, G., Sutera, A., Vulpiani, A.: A theory of stochastic resonance in climatic change. SIAM J. Appl. Math. **43**, 565–578 (1983)
4. Huelga, S.F., Plenio, M.B.: Stochastic resonance phenomena in quantum many-body systems. Phys. Rev. Lett. **98**, 170601 (2007)
5. Zhong, W.R., Shao, Y.Z., He, Z.H.: Pure multiplicative stochastic resonance of a theoretical anti-tumor model with seasonal modulability. Phys. Rev. E **73**, 060902 (2006)
6. Hirano, Y., Segawa, Y., Kawai, T., Matsumoto, T.: Stochastic resonance in a molecular redox circuit. J. Phys. Chem. C **117**, 140–145 (2013)
7. Mondal, D., Muthukumar, M.: Stochastic resonance during a polymer translocation process. J. Chem. Phys. **144**, 144901 (2016)
8. Valenti, D., Fiasconaro, A., Spagnolo, B.: Stochastic resonance and noise delayed extinction in a model of two competing species. Physica A **331**, 477–486 (2004)
9. Hänggi, P.: Stochastic resonance in biology. How noise can enhance detection of weak signals and help improve biological information processing. ChemPhysChem **3**, 285–290 (2002)
10. McDonnell, M.D., Abbott, D.: What is stochastic resonance? Definitions, misconceptions, debates, and its relevance to biology. PLoS Comput. Biol. **5**, e1000348 (2009)
11. Berdichevsky, V., Gitterman, M.: Multiplicative stochastic resonance in linear systems: analytical solution. Europhys. Lett. **36**, 161–165 (1996)

12. Jia, Y., Yu, S.N., Li, J.R.: Stochastic resonance in a bistable system subject to multiplicative and additive noise. Phys. Rev. E **62**, 1869–1878 (2000)

13. Zheng, R., Nakano, K., Hu, H., Su, D., Cartmell, M.P.: An application of stochastic resonance for energy harvesting in a bistable vibrating system. J. Sound Vib. **333**, 2568–2587 (2014)

14. Mitaim, S., Kosko, B.: Adaptive stochastic resonance. Proc. IEEE **86**, 2152–2183 (1998)

15. Mitaim, S., Kosko, B.: Adaptive stochastic resonance in noisy neurons based on mutual information. IEEE Trans. Neural Netw. **15**, 1526–1540 (2004)

16. Lei, Y., Han, D., Lin, J., He, Z.: Planetary gearbox fault diagnosis using an adaptive stochastic resonance method. Mech. Syst. Signal Process. **38**, 113–124 (2013)

17. Collins, J.J., Chow, C.C., Imhoff, T.T.: Aperiodic stochastic resonance in excitable systems. Phys. Rev. E **52**, R3321 (1995)

18. Collins, J.J., Chow, C.C., Capela, A.C., lmhoff, T.T.: Aperiodic stochastic resonance. Phys. Rev. E **54**, 5575–5584 (1996)

19. Collins, J.J., Chow, C.C., Imhoff, T.T.: Stochastic resonance without tuning. Nature **376**, 236–238 (1995)

20. Kohar, V., Sinha, S.: Noise-assisted morphing of memory and logic function. Phys. Lett. A **376**, 957–962 (2012)

21. Duan, F., Rousseau, D., Chapeau-Blondeau, F.: Residual aperiodic stochastic resonance in a bistable dynamic system transmitting a suprathreshold binary signal. Phys. Rev. E **69**, 011109 (2004)

22. Duan, F., Abbott, D.: Binary modulated signal detection in a bistable receiver with stochastic resonance. Physica A **376**, 173–190 (2007)

23. Liu, J., Li, Z., Guan, L., Pan, L.: A novel parameter-tuned stochastic resonator for binary PAM signal processing at low SNR. IEEE Commun. Lett. **18**, 427–430 (2014)

24. Liu, J., Li, Z.: Binary image enhancement based on aperiodic stochastic resonance. IET Image Process. **9**, 1033–1038 (2015)

25. Collins, J.J., Imhoff, T.T., Grigg, P.: Noise-enhanced information transmission in rat SA1 cutaneous mechanoreceptors via aperiodic stochastic resonance. J. Neurophysiol. **76**, 642–645 (1996)

26. Sun, S., Lei, B.: On an aperiodic stochastic resonance signal processor and its application in digital watermarking. Signal Process. **88**, 2085–2094 (2008)

27. Li, X., Cao, G., Liu, H.: Aperiodic signals processing via parameter-tuning stochastic resonance in a photorefractive ring cavity. AIP Adv. **4**, 047111 (2014)

28. Barbay, S., Giacomelli, G., Marin, F.: Experimental evidence of binary aperiodic stochastic resonance. Phys. Rev. Lett. **85**, 4652–4655 (2000)

29. Barbay, S., Giacomelli, G., Marin, F.: Stochastic resonance in vertical cavity surface emitting lasers. Phys. Rev. E **61**, 157–166 (2000)

30. Barbay, S., Giacomelli, G., Marin, F.: Noise-assisted transmission of binary information: theory and experiment. Phys. Rev. E **63**, 051110 (2001)

31. Chizhevsky, V.N., Giacomelli, G.: Vibrational resonance and the detection of aperiodic binary signals. Phys. Rev. E **77**, 051126 (2008)

32. Hu, G., Gong, D., Yang, C., Qing, G., Li, R.: Stochastic resonance in a nonlinear system driven by an aperiodic force. Phys. Rev. A **46**, 3250–3254 (1992)

33. Yu, T., Zhang, L., Luo, M.K.: Stochastic resonance in the fractional Langevin equation driven by multiplicative noise and periodically modulated noise. Phys. Scr. **88**, 045008 (2013)

34. Litak, G., Borowiec, M.: On simulation of a bistable system with fractional damping in the presence of stochastic coherence resonance. Nonlinear Dyn. **77**, 681–686 (2014)

35. Zhong, S., Ma, H., Peng, H., Zhang, L.: Stochastic resonance in a harmonic oscillator with fractional-order external and intrinsic dampings. Nonlinear Dyn. **82**, 535–545 (2015)

36. Monje, C.A., Vinagre, B.M., Feliu, V., Chen, Y.: Tuning and auto-tuning of fractional order controllers for industry applications. Control Eng. Pract. **16**, 798–812 (2008)

37. Bohannan, G.W.: Analog fractional order controller in temperature and motor control applications. J. Vib. Control **14**, 1487–1498 (2008)

38. Diethelm, K., Freed, A.D.: On the solution of nonlinear fractional-order differential equations used in the modeling of viscoplasticity. In: Keil, F., Mackens, W., Voß, H., Werther, J. (eds.) Scientific Computing in Chemical Engineering II, pp. 217–224. Springer, Berlin (1999)

39. Meral, F.C., Royston, T.J., Magin, R.: Fractional calculus in viscoelasticity: an experimental study. Commun. Nonlinear Sci. Numer. Simul. **15**, 939–945 (2010)

40. Sheng, H., Chen, Y., Qiu, T.: Fractional Processes and Fractional-Order Signal Processing: Techniques and Applications. Springer, London (2011)

41. Yau, H.T., Wu, S.Y., Chen, C.L., Li, Y.C.: Fractional-Order chaotic self-synchronization-based tracking faults diagnosis of ball bearing systems. IEEE Trans. Ind. Electron. **63**, 3824–3833 (2016)

42. Craiem, D., Magin, R.L.: Fractional order models of viscoelasticity as an alternative in the analysis of red blood cell (RBC) membrane mechanics. Phys. Biol. **7**, 013001 (2010)

43. Shen, Y.J., Wei, P., Yang, S.P.: Primary resonance of fractional-order van der Pol oscillator. Nonlinear Dyn. **77**, 1629–1642 (2014)

44. Shen, Y.J., Wei, P., Sui, C.Y., Yang, S.P.: Subharmonic resonance of van der Pol oscillator with fractional-order derivative. Math. Probl. Eng. **2014**, 738087 (2014)

45. Yang, J.H., Zhu, H.: Vibrational resonance in Duffing systems with fractional-order damping. Chaos **22**, 013112 (2012)

46. Petráš, I.: Fractional-Order Nonlinear Systems: Modeling, Analysis and Simulation. Higher Education Press, Beijing (2011)

47. Monje, C.A., Chen, Y.Q., Vinagre, B.M., Xue, D., Feliu, V.: Fractional-Order Systems and Controls: Fundamentals and Applications. Springer, London (2010)

48. Nayfeh, A.H., Balachandran, B.: Applied Nonlinear Dynamics: Analytical, Computational and Experimental Methods. Wiley, Weinheim (2008)

49. Thompson, J.M.T., Stewart, H.B.: Nonlinear Dynamics and Chaos. Wiley, New York (2002)

50. Yang, J.H., Sanjuán, M.A.F., Liu, H.G., Litak, G., Li, X.: Stochastic P-bifurcation and stochastic resonance in a noisy bistable fractional-order system. Commun. Nonlinear Sci. **41**, 104–117 (2016)

51. Zhu, W.Q.: Random Vibration, pp. 371–372. Science Press, Beijing (1992)
52. Poli, R., Kennedy, J., Blackwell, T.: Particle swarm optimization. Swarm Intell. **1**, 33–57 (2007)
53. Eberhart, R.C., Shi, Y.: Particle swarm optimization: developments, applications and resources. In: Proceeding of IEEE Congress on Evolutionary Computation, pp. 81–86. Seoul, Korea (2001)
54. Deb, K., Pratap, A., Agarwal, S., Meyarivan, T.: A fast and elitist multiobjective genetic algorithm: NSGA-II. IEEE Trans. Evol. Comput. **6**, 182–197 (2002)
55. Zhan, Z.H., Zhang, J., Li, Y., Chung, H.S.H.: Adaptive particle swarm optimization. IEEE Trans. Syst. Man Cybern. B **39**, 1362–1381 (2009)